

Supplementary Information

Thermoelectric Properties of $(\text{In}, \text{Cr})_2\text{Ge}_2\text{Te}_6$ Layered Compounds

Chenxi Xu^{1,2}, Hexige Wuliji^{3}, Pengfei Qiu¹, Kunpeng Zhao^{4*}, and Xun Shi^{1,2*}*

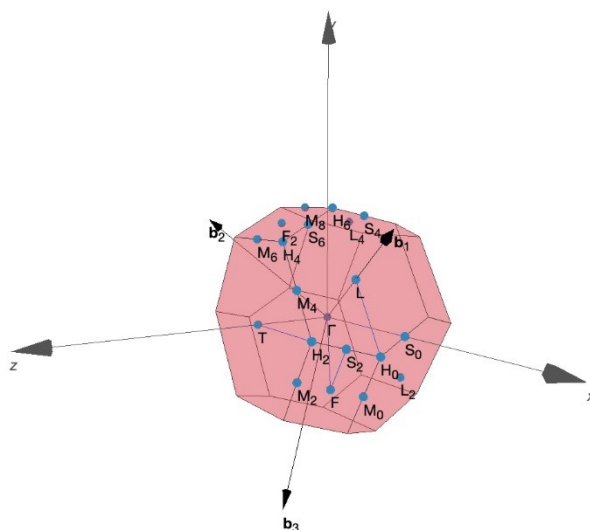


Figure S1. The Brillouin zone of $\text{In}_2\text{Ge}_2\text{Te}_6$ or $\text{Cr}_2\text{Ge}_2\text{Te}_6$.

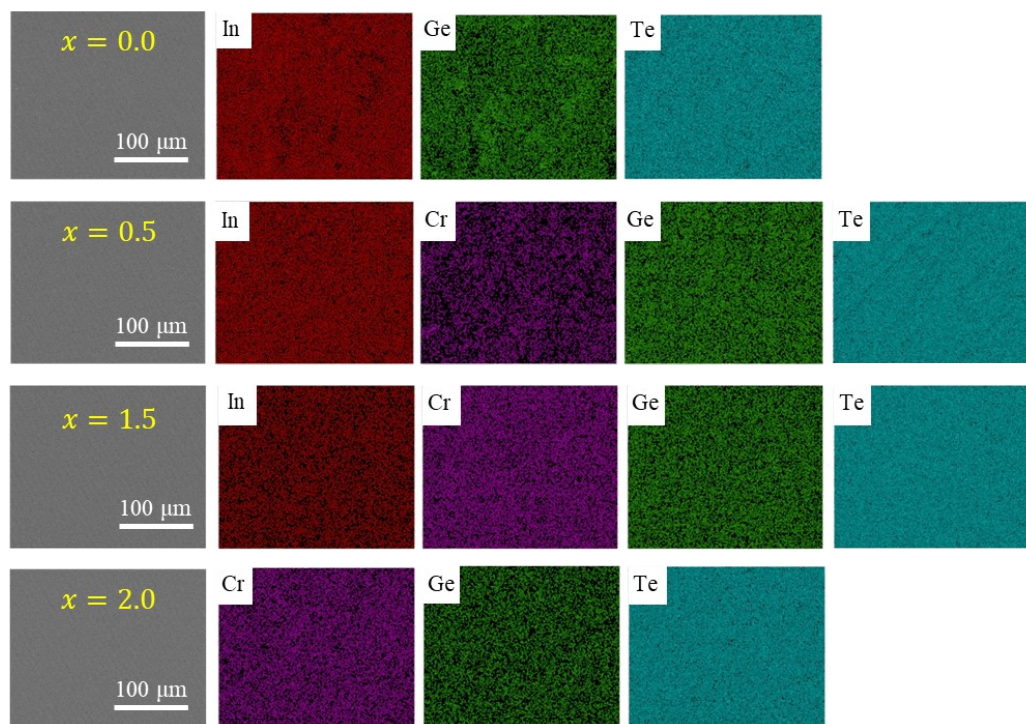


Figure S2. Backscattered electron (BSE) images and corresponding energy dispersive

X-ray spectroscopy (EDS) mappings for $\text{In}_{2-x}\text{Cr}_x\text{Ge}_2\text{Te}_6$ ($x = 0.0, 0.5, 1.5, 2.0$).

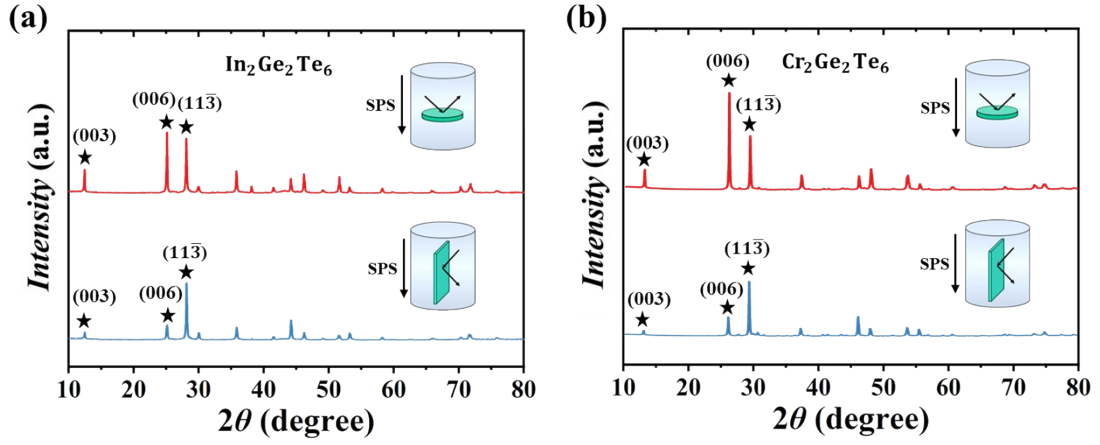


Figure S3. Room temperature X-ray diffraction (XRD) patterns for bulk (a) $\text{In}_2\text{Ge}_2\text{Te}_6$ and (b) $\text{Cr}_2\text{Ge}_2\text{Te}_6$.

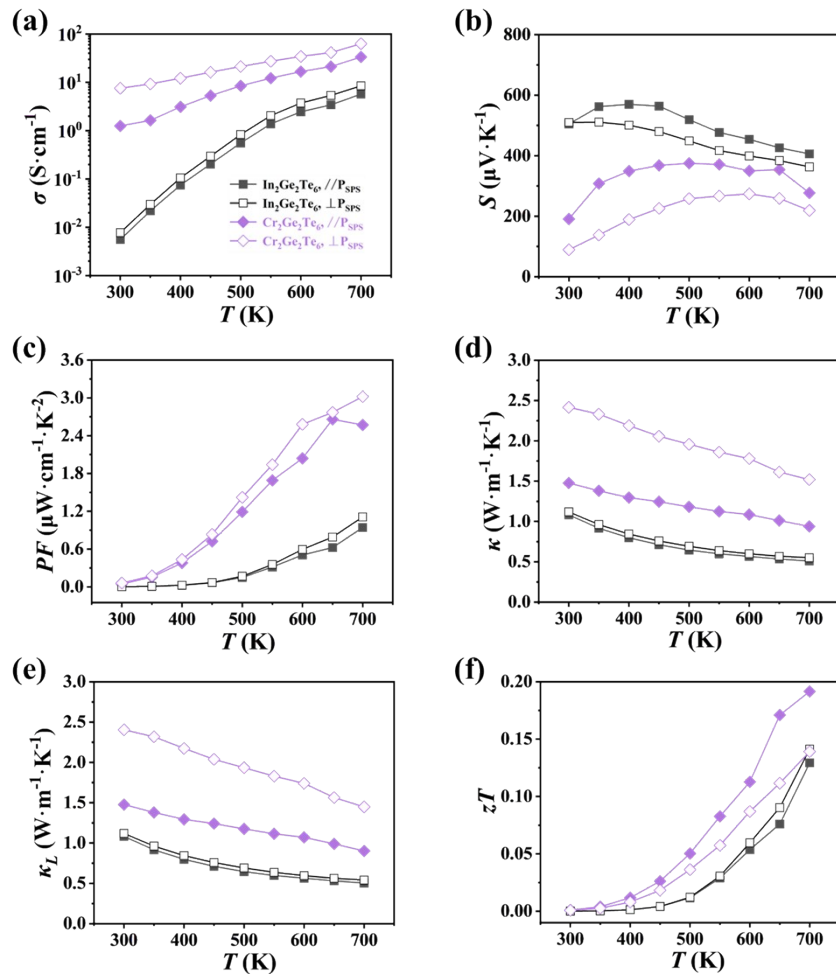


Figure S4. Temperature dependence of thermoelectric properties for $\text{In}_2\text{Ge}_2\text{Te}_6$ and

$\text{Cr}_2\text{Ge}_2\text{Te}_6$ parallel ($//$) and perpendicular (\perp) to the SPS pressing direction. **(a)** Electrical conductivity σ , **(b)** Seebeck coefficient S , **(c)** power factor PF , **(d)** total thermal conductivity κ , **(e)** lattice thermal conductivity κ_L and **(f)** TE figure of merit zT .

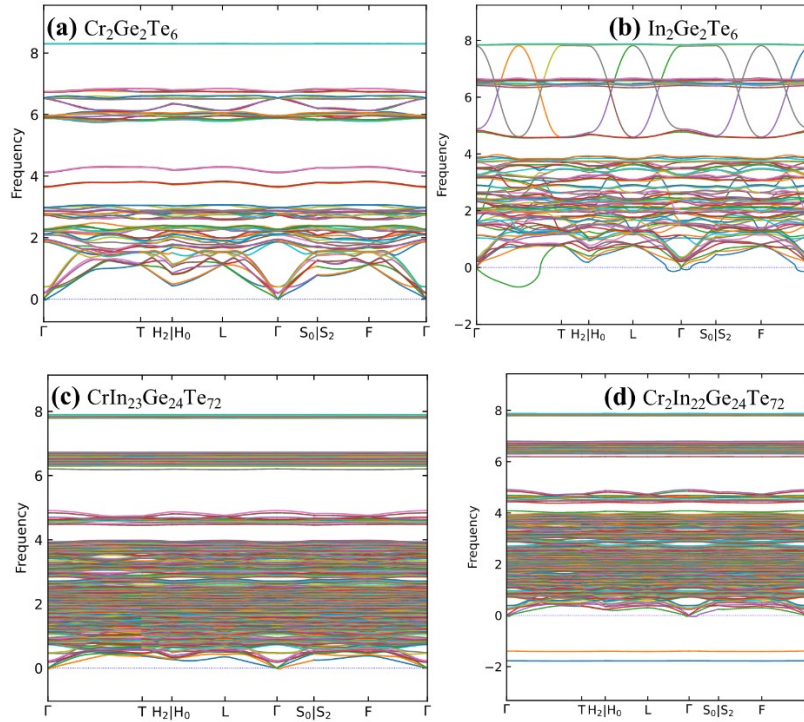


Figure S5. Phonon dispersions obtained from hiPhive and phonopy packages for (a) $\text{Cr}_2\text{Ge}_2\text{Te}_6$, (b) $\text{In}_2\text{Ge}_2\text{Te}_6$, (c) $\text{CrIn}_{23}\text{Ge}_{24}\text{Te}_{72}$, (d) $\text{Cr}_2\text{In}_{22}\text{Ge}_{24}\text{Te}_{72}$.

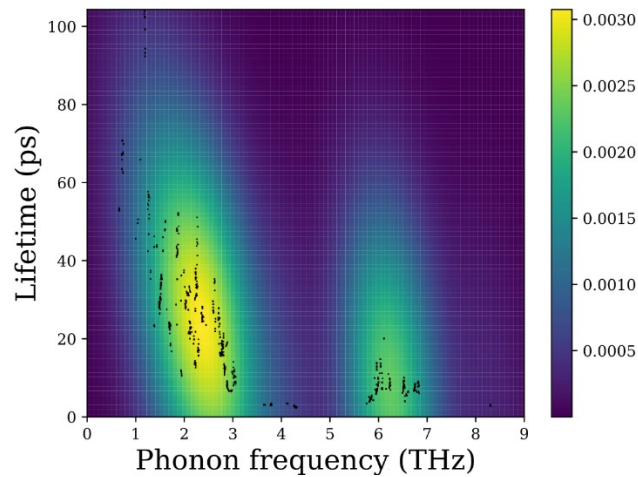


Figure S6. Calculated phonon lifetimes as a function of phonon frequency for $\text{Cr}_2\text{Ge}_2\text{Te}_6$ at 300 K. The color bar indicates the density of phonon modes estimated via

Gaussian Kernel Density Estimation (KDE), where brighter regions represent a higher concentration of modes. The superimposed black dots represent the raw mode-resolved data.

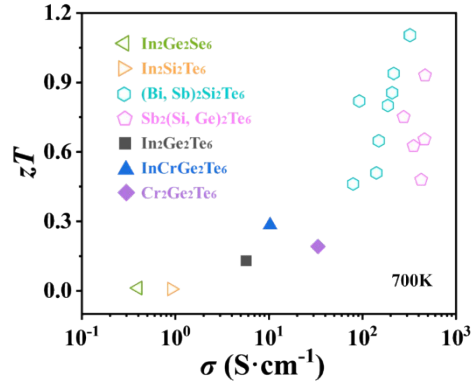


Figure S7. zT values as a function of electrical conductivity for $M_2N_2Q_6$ -type layered compounds.^[1-7]

Table S1. The calculated Lorenz number L of $In_{2-x}Cr_xGe_2Te_6$. The unit of the Lorenz number L is $10^{-8} V^2 \cdot K^{-2}$.

T (K)	L ($x = 0.0$)	L ($x = 0.5$)	L ($x = 1.0$)	L ($x = 1.5$)	L ($x = 2.0$)
300	1.51286	1.81773	1.56732	1.50179	1.69271
350	1.50787	1.71557	1.51929	1.50196	1.57029
400	1.50734	1.63888	1.50623	1.50222	1.54936
450	1.50773	1.57338	1.50486	1.50381	1.5419
500	1.5114	1.53979	1.50534	1.50618	1.53945
550	1.51637	1.5302	1.5085	1.50896	1.54083
600	1.51996	1.52818	1.50935	1.51355	1.54894
650	1.52542	1.53349	1.51652	1.51847	1.54728
700	1.5302	1.53527	1.52586	1.52794	1.59182
750	1.53527

Table S2. Reciprocal space and Brillouin-zone information

Reciprocal cell vectors (1/Å)			
b	x	y	z
b ₁	0.9101304292	0.5254640483	0.2911091454
b ₂	-0.9101304292	0.5254640483	0.2911091454
b ₃	0.0000000000	-1.0509280966	0.2911091454
Suggested path			
Γ—T—H ₂ H ₀ —L—Γ—S ₀ S ₂ —F—Γ			
High-symmetry points (scaled units)			
Label	k1	k2	k3
F	0.5000000000	0.0000000000	0.5000000000
F ₂	0.5000000000	0.5000000000	0.0000000000
Γ	0.0000000000	0.0000000000	0.0000000000
H ₀	0.5000000000	-0.2178200582	0.2178200582
H ₂	0.7821799418	0.2178200582	0.5000000000
H ₄	0.7821799418	0.5000000000	0.2178200582
H ₆	0.5000000000	0.2178200582	-0.2178200582
L	0.5000000000	0.0000000000	0.0000000000
L ₂	0.0000000000	-0.5000000000	0.0000000000
L ₄	0.0000000000	0.0000000000	-0.5000000000
M ₀	0.3589100291	-0.2178200582	0.3589100291
M ₂	0.6410899709	0.2178200582	0.6410899709
M ₄	0.7821799418	0.3589100291	0.3589100291
M ₆	0.6410899709	0.6410899709	0.2178200582
M ₈	0.3589100291	0.3589100291	-0.2178200582
S ₀	0.3589100291	-0.3589100291	0.0000000000
S ₂	0.6410899709	0.0000000000	0.3589100291
S ₄	0.3589100291	0.0000000000	-0.3589100291
S ₆	0.6410899709	0.3589100291	0.0000000000

T	0.5000000000	0.5000000000	0.5000000000
---	--------------	--------------	--------------

Table S3. The calculated lattice thermal conductivity κ_L of $\text{In}_{2-x}\text{Cr}_x\text{Ge}_2\text{Te}_6$. The unit of κ_L is $\text{W}\cdot\text{m}^{-1}\cdot\text{K}^{-1}$.

T (K)	κ_L ($x = 0.0$)	κ_L ($x = 0.5$)	κ_L ($x = 1.0$)	κ_L ($x = 1.5$)	κ_L ($x = 2.0$)
300	1.08269	0.72917	0.85272	1.02198	1.47686
350	0.9157	0.65005	0.76252	0.93701	1.3791
400	0.79773	0.58695	0.69686	0.86326	1.29407
450	0.71149	0.5371	0.63929	0.80202	1.24131
500	0.64495	0.49502	0.59373	0.74884	1.17548
550	0.59783	0.46588	0.55316	0.70926	1.11463
600	0.56362	0.44017	0.51596	0.68318	1.07046
650	0.53065	0.3988	0.47611	0.618	0.98965
700	0.50408	0.34963	0.44544	0.56263	0.90173
750	0.42839

Table S4. Transverse (v_T), longitudinal (v_L) and average sound velocity (v_S) of $\text{In}_{2-x}\text{Cr}_x\text{Ge}_2\text{Te}_6$ parallel (\parallel) and perpendicular (\perp) to the SPS pressing direction. The unit

of sound velocity is $\text{m}\cdot\text{s}^{-1}$;
$$v_S = \left[\frac{1}{3} \left(\frac{2}{v_T^3} + \frac{1}{v_L^3} \right) \right]^{-1/3}$$
.

sample	direction	v_T	v_L	v_S
$x = 0.0$	parallel	1452	2573	1615
	perpendicular	1709	2842	1891
$x = 0.5$	parallel	1580	2772	1756
$x = 1.0$	parallel	1660	2853	1841
$x = 1.5$	parallel	1645	2880	1828
$x = 2.0$	parallel	1521	2722	1693
	perpendicular	1783	3206	1985

Table S5. Calculated lattice thermal conductivities in different directions for $\text{Cr}_2\text{Ge}_2\text{Te}_6$.

T (K)	xx	yy	zz
100	21.290	24.561	13.461
200	9.994	11.484	6.313
300	6.575	7.549	4.154
400	4.908	5.633	3.101

Table S6. Room temperature electrical properties of $\text{In}_{2-x}\text{Cr}_x\text{Ge}_2\text{Te}_6$

	S ($\mu\text{V} \cdot \text{K}^{-1}$)	σ ($\text{S} \cdot \text{cm}^{-1}$)	μ_w ($\text{cm}^2 \cdot \text{V}^{-1} \cdot \text{s}^{-1}$)
$x = 0.0$	505	0.0056	0.0873
$x = 0.5$	133	0.0165	0.0034
$x = 1.0$	292	0.0169	0.0223
$x = 1.5$	734	0.0232	5.1472
$x = 2.0$	191	1.2531	0.5141

References

- [1] L. Lu, P. Li, T. Wu, et al., Atomic-scale structure and properties of a new layered ternary selenide semiconductor $\text{In}_2\text{Ge}_2\text{Se}_6$, *Materials Characterization* 230 (2025): 115835.
- [2] T. Suriwong, K. Kurosaki, S. Thongtem, Thermoelectric properties of phosphorus-doped indium tellurosilicate: InSiTe_3 , *J. Alloys Compd.* 735 (2018) 75-80.
- [3] Y. Luo, Z. Ma, S. Hao, et al., Thermoelectric Performance of the 2D $\text{Bi}_2\text{Si}_2\text{Te}_6$ Semiconductor, *J. Am. Chem. Soc.* 144 (3) (2022) 1445-1454.
- [4] Y. Luo, S. Cai, S. Hao, et al., High-performance thermoelectrics from cellular nanostructured $\text{Sb}_2\text{Si}_2\text{Te}_6$, *Joule* 4 (1) (2020) 159-175.
- [5] C. Chen, D. Shen, C. Xia, et al., Integrating band engineering with point defect scattering for high thermoelectric performance in $\text{Bi}_2\text{Si}_2\text{Te}_6$, *Chem. Eng. J.* 441 (2022): 135968.
- [6] K. Saglik, X. Wang, X. Tan, et al., High Entropy Bi-Ti Alloying for Improved $\text{Sb}_2\text{Si}_2\text{Te}_6$ Thermoelectrics, *Adv. Eng. Mater.* 27 (2025): 2500380.
- [7] W. Wang, X. Lu, L. Sun, et al., Enhancing the thermoelectric performance of $\text{Sb}_2\text{Si}_2\text{Te}_6$ by germanium doping, *J. Mater. Chem. A* 10 (2022) 20489-20496.